Strain Control of Domain-Wall Stability in Epitaxial $BiFeO_3$ (110) Films

M. P. Cruz,[1,2] Y. H. Chu,[1,*] J. X. Zhang,[3] P. L. Yang,[1] F. Zavaliche,[1] Q. He,[1] P. Shafer,[1] L. Q. Chen,[3] and R. Ramesh[1]

[1]*Department of Materials Science and Engineering, and Department of Physics, University of California, Berkeley, California 94720, USA*

[2]*Centro de Ciencias de la Materia Condensada, Universidad Nacional Autónoma de México, Km 107, Carretera Tijuana-Ensenada, Ensenada B.C., México, C.P 22800*

[3]*Department of Materials Science and Engineering, Pennsylvania State University, University Park, Pennsylvania 16802, USA*

(Received 10 May 2007; published 20 November 2007)

We have studied the stability of domains and domain walls in multiferroic $BiFeO_3$ thin films using a combination of piezoelectric force microscopy and phase-field simulations. We have discovered that a film-substrate misfit strain may result in a drastically different thermodynamic stability of two parallel domain walls with the same orientation. A fundamental understanding of the underlying physics, the stress distribution in a domain structure, leads to a novel approach to control the ferroelastic domain stability in the multiferroic $BiFeO_3$ system.

DOI: 10.1103/PhysRevLett.99.217601 PACS numbers: 77.80.Fm, 68.37.Ps, 75.80.+q, 77.80.Dj

Multiferroics, or materials that simultaneously show magnetic and ferroelectric order, hold the promise of coupling between magnetic and electric order parameters [1–3]. While the phenomenon is by itself of fundamental importance, the possibility for control of magnetic properties with an electric field (and vice versa) is of significant interest for applications in high frequency devices, storage media, and electric field control of spintronics. The cross correlation between magnetic and electric domains has been observed by optical techniques in one model multiferroic, $YMnO_3$ [2]. The stability of switched (written) domains against time is one of the critical issues for applications of multiferroics. It is well understood that favorable domain-wall configurations correspond to those having low wall energy that satisfies the electrical, magnetic, and mechanical compatibility conditions. A basic understanding of the distributions of electric, magnetic, and stress fields within domain structures allows one to manipulate the relative stability of domains and domain walls. This work explores the effect of substrate-film mismatch strain on internal stress distributions within domain structures and thus the domain stability and domain-wall motion in multiferroic $BiFeO_3$ (BFO) thin films. Such an approach is rather general and can be employed to control the stability of other ferroic systems [4,5].

BFO is a room-temperature antiferromagnet and ferroelectric with transition temperatures of $\sim 370\,^{\circ}C$ [6] and $\sim 820\,^{\circ}C$ [7], respectively. Its crystalline structure is rhombohedral with a spontaneous electric polarization of $\sim 90\ \mu C/cm^2$ directed along the pseudocubic $\langle 111 \rangle$ of the base perovskite unit [8,9]. The magnetic moments are coupled ferromagnetically within the (111) planes and antiferromagnetically between the (111) planes perpendicular to the polarization direction [10]. Consequently, a non-180° rotation of the ferroelectric polarization may change the orientation of the easy magnetization plane. The possibility of coupling between antiferromagnetism and the ferroelectric polarization and changing it through an electric field induced switching of the polarization has been demonstrated [11]. Specifically, it appears that controlled 109° rotation of the ferroelectric polarization may be useful in terms of stimulating a corresponding change in the direction of antiferromagnetic order. Therefore, it is critical to understand approaches that will lead to stable, electrically controllable 109° rotation of the ferroelectric polarization. In order to simplify the domain structure, we have used a (110) orientation for the BFO thin film in which we demonstrate the control and stability of 109° ferroelastic switching using piezoelectric force microscopy (PFM) [10,11].

BFO films were synthesized by pulsed laser deposition (PLD) at 700 °C in 100 mTorr of oxygen. $SrRuO_3$ bottom electrodes, 50-nm thick, were deposited by PLD on $SrTiO_3$ (STO) substrates with (110) orientation [12]. The ferroelectric domain structure of the films was reconstructed using the approach described before [13–15] based on the out-of-plane (OP) and in-plane (IP) PFM contrast. A DI MultiMode scanning probe microscope with a Nanoscope IV controller was used for this purpose. An ac bias of 2.0 Vpp at 6.39 kHz was applied to the tip for imaging. The switching and relaxation of this ferroelectric domain structure under a substrate constraint is modeled using the phase-field method [16], in which the spatial distribution of the polarization field and its evolution are described by the time-dependent Ginzburg-Landau (TDGL) equations [17].

The switching behavior in BFO films depends on the substrate orientation and the consequent domain structures in the film. For example, only 180° polarization reversal is observed in single-domain (111) films. Conversely, in a polydomain BFO(001) film, all three possible ferroelectric switching mechanisms have been observed [14]. Moreover, higher applied fields increase the propensity for ferroelastic switching. Using the voltage to selectively activate ferroelectric or ferroelastic switching provides a

pathway to control the spatial distribution of antiferromagnetism. Because the domain structure of BFO(001) is complicated by the presence of several polarization variants [14], we have used the (110) orientation to demonstrate selectivity of the switching mechanism. The typical as-grown state of (110)-oriented BFO films is characterized by two polarization variants (P^-_1 and P^-_2) pointing towards the bottom electrode and separated by 71°. All the switching studies were carried out well within each of these two domain variants shown in Fig. 1(b). These experiments use the crystallography of the substrate as a reference [described in Fig. 1(a)]; further, all of the results described here are based on scans where [1$\bar{1}$0] and [001] are the fast and slow scanning directions, respectively, of the AFM cantilever. The displacement of the tip is indicated in the red arrows in Fig. 1(d).

When a negative voltage is applied through the AFM tip to this initial state, we can expect the following two possibilities for switching. The first is that P^-_1 switches to P^+_1, corresponding to a 180° polarization reversal [Fig. 1(a)]. The other pathway is one in which P^-_1 switches to P^+_2, corresponding to a 109° rotation of the polarization [Fig. 1(a)]. Phase-field simulations were carried out to explore the thermodynamic stability of these two switching mechanisms. The simulation results suggest that ferroelectric or ferroelastic switching can be selected by the magnitude of the applied field; lower fields favor 180° switching while at higher fields 109° switching is predicted. Our experimental results confirm these predictions; for 120 nm BFO films, 180° switching occurred at tip bias from −5 to −8 V, as evidenced by the uniform white IP tone and dark OP tone in Fig. 1(c). Applying higher negative biases, i.e., −10 to −20 V, resulted in 109° switching, as deduced from the IP [Fig. 1(d)] and OP-PFM images [similar to the inset in Fig. 1(c)]. Finally, we note that when a large positive bias (20–26 V) is applied to the initial state, P^-_1, we observe a 71° change in the polarization direction from P^-_1 to P^-_2 [Fig. 1(e)]; although this is unexpected, it can be understood as a consequence of an in-plane component of the electric field that acts on P^-_1. A 180° sample rotation was also performed: no switching was observed, which confirms our hypothesis that the switching observed at large positive bias is indeed due to an in-plane component of the electric field.

We now focus on the dynamics of ferroelastic 109° switching within the framework shown schematically in Fig. 2(a). A square region (shaded yellow) that has been switched by 109° is characterized by four domain walls (I, II, III, and IV); I and III correspond to (001)-type interfaces while II and IV correspond to (110)-type interfaces. We observe that this square region begins to relax by a sub-

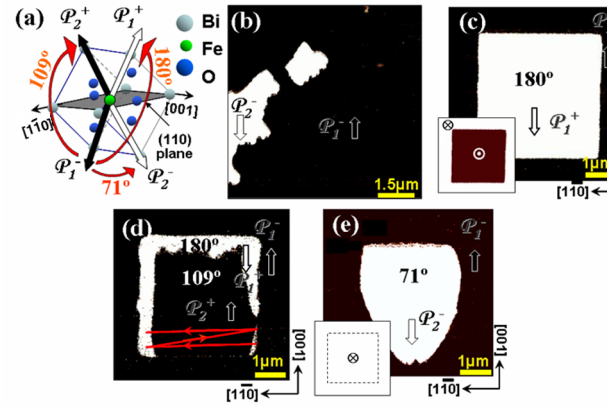

FIG. 1 (color online). (a) Schematics of the polarization variants observed in as-grown BFO(110) film and corresponding possible switching events. (b) IP-PFM image showing the two domain variants. IP-PFM images of the BFO(110) film after PFM poling at (c) lower negative voltage, (d) higher negative voltage, and (e) high positive voltage. The insets in (c) and (e) are the corresponding OP-PFM images.

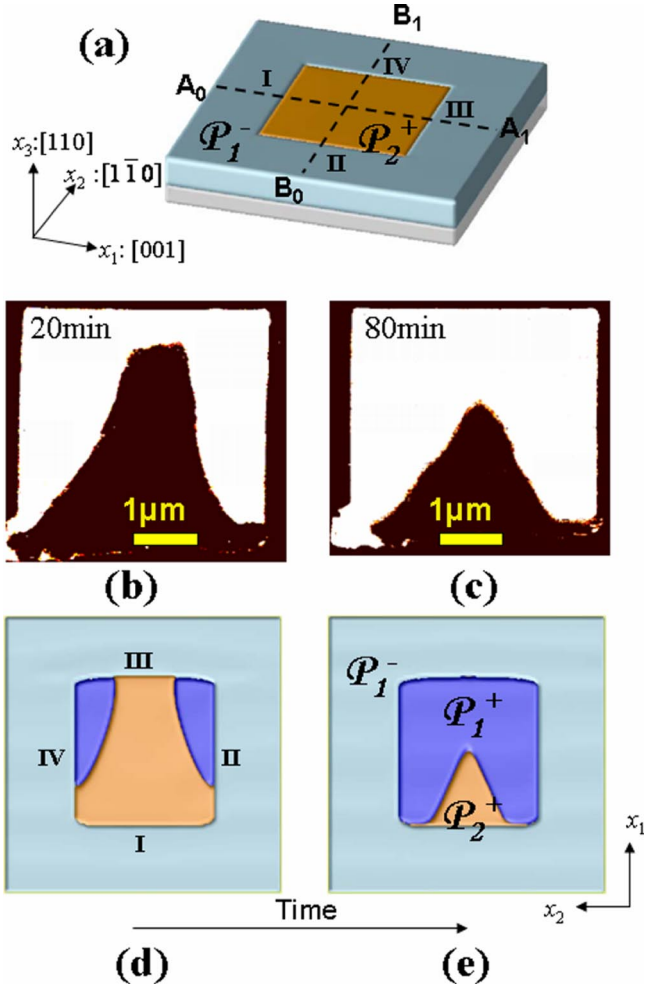

FIG. 2 (color online). (a) Schematics of as-grown (blue) and poled (orange) film on substrate. Relaxation of a ferroelastically switched region at different time regime (b) 20 min and (c) 80 min. [Initial state: P_1^-, applied voltage (−18 V)]; (d), (e) the corresponding phase-field simulation of the relaxation.

sequent 71° reversal, which is captured at two different times in Figs. 2(b) and 2(c)]; such a 71° relaxation ultimately covers the entire area that was originally switched. It is noteworthy that the relaxation process is not uniform over this area; instead, relaxation progresses rapidly from II, III, and IV, while interface I is very stable.

This relaxation process is a consequence of replacing the high elastic energy of the 109° domain walls created during the poling process with less stressed 180° domain walls. As shown by Streiffer, *et al.* [4], the domain walls satisfying the elastic compatibility condition for the $P^-{}_1/P^+{}_2$ variant pairs are (001)-type and (110)-type planes. Therefore, the domain walls II and IV have large elastic energy due to the mismatched deformation along the walls and are expected to relax rapidly. However, it is interesting to note the difference in the stability of domain walls I and III, even though they correspond to the same (001)-type plane. Relaxation measurements of BFO films with different thicknesses (120 nm–800 nm) suggest that the lattice mismatch between the film and substrate affects the relative stability of the four domain walls. X-ray diffraction measurements confirmed that the strain state is released when the film thickness is increased to 800 nm. The area of 109° domain and the corresponding domain-wall length as a function of time, plotted in Fig. 3, clearly shows that the relaxation speed of 109° domain walls in thicker BFO films is much slower. In order to verify the substrate natural miscut effect, we have also performed the same experiments on the other initial state, i.e., $P_2{}^-$. Therefore, also shown in this figure are the relaxation data for the two types of initial domains ($P_1{}^-$ and $P_2{}^-$) that are observed in this type of sample [described in Fig. 1(a) and 1(b)]. The relaxation processes for these two types of initial domains are essentially the same as this figure shows.

To clarify the nondegeneracy of walls I and III, the calculated stress distribution along the A_0-A_1 cross section of the film is plotted in Fig. 4(a). This stress in the film can be subdivided into two contributions: (a) the lattice mismatch between the film and substrate along the film-substrate interface, and (b) accommodation of the differing spontaneous strains of the polarization variants at domain walls [5]. Even without the substrate-induced stress, there are still large nonuniform stresses in the film [Fig. 4(b)] to maintain coherency along the domain walls and the film-substrate interface. We note that at domain walls I and III the in-plane stress (σ_{11}) distributions are essentially the same except for the sign, and the distributions of other stress components (σ_{13} and σ_{33}) are either the same or different only in the sign (not shown); therefore, in the absence of epitaxial stress, equal elastic energies are expected for the two domain walls. However, for the BFO film studied here, the mismatch between the film and STO substrate adds a significant in-plane compressive stress (σ_{11}), so that the tensile stress near domain wall I was compensated, while the compressive stress near domain interface III was considerably increased. As a result, the elastic energies of domain walls I and III are not equivalent, and domain wall III has larger elastic energy especially near the junction with the film surface. The phase-field simulations show that the relaxation process starts from the domain walls with higher elastic energy, i.e., domain II, IV, and to a lesser extent, III [Figs. 2(d) and 2(e)], all in excellent agreement with experimental observation [Figs. 2(b) and 2(c)]. Therefore, the stability of domain wall III can be enhanced by decreasing the substrate-induced compressive stress (strain). Phase-field simulations also demonstrate a slower relaxation process

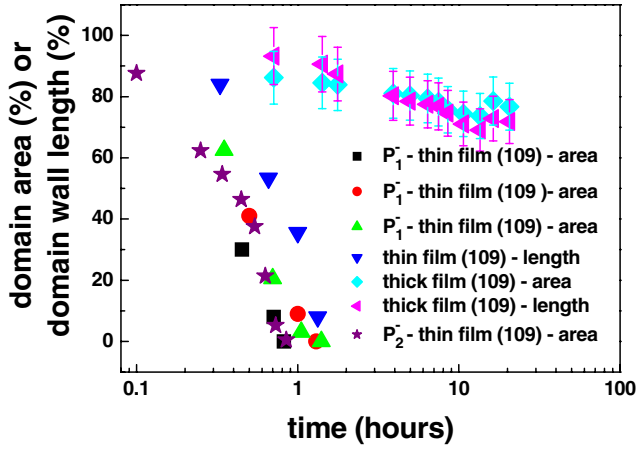

FIG. 3 (color online). The domain area and the corresponding domain-wall length as a function of relaxation time with different film thickness (120 nm for thin film and 800 nm for thick film). Also shown in this figure is the relaxation data for the two types of initial domains ($P_1{}^-$ and $P_2{}^-$). Note that the relaxation behaviors for both are quite similar.

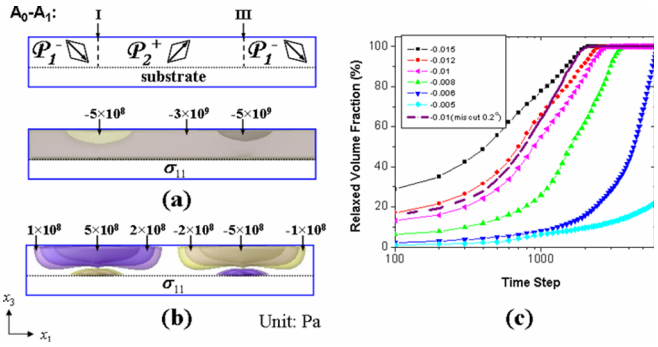

FIG. 4 (color online). Phase-field simulations of BFO/STO(110) depicting (a) the total stress distribution in the film, (b) the component of the stress distribution resulting only from the boundary conditions of the domain walls (ignoring substrate lattice mismatch), and (c) the relaxed volume as a function of time with different strain state. The broken line (—) curve is a calculation of the relaxation of a film that has a structural bias (vicinal cut) of 0.2°.

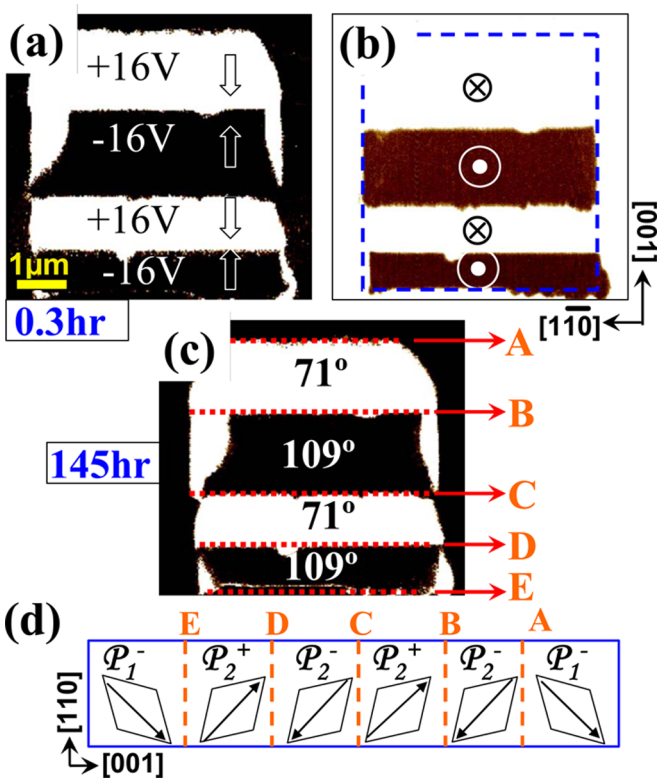

FIG. 5 (color online). (a) IP- and (b) OP-PFM images after poling the sample along [001] (slow-scan direction) while alternating the bias between −16 and +16 V. (c) The same as in (a) but after 145 h. (d) Cross-sectional ($1\bar{1}0$) schematic of the polarization variants in each domain.

for smaller substrate-induced strains [Fig. 4(c)]. Furthermore, preliminary calculations indicate that for a vicinal angle of 0.2° the relaxation process does progress faster [Fig. 4(c)], although this is not a dramatic change from the nonvicinal sample; i.e., the overall trend is still the same. We are now pursuing the systematic effects of different vicinal angles (0°–5°) on the switching and subsequent relaxation behavior, both experimentally and theoretically.

We now address the critical issue with respect to magnetoelectric coupling: demonstrating that the 109° as-switched state can be dramatically stabilized through a purposeful engineering of the domain-wall architecture. The key conclusions from the data in Figs. 2 and 4 show that walls of type I are very stable to perturbations. We use these walls to anchor the domain structure in the written regions and have exploited this selective stability by alternating the sign of the poling bias applied to contiguous, rectangular regions of the film, while maintaining a continuous raster pattern. Figure 5 shows the domain structure of a square region poled in this manner with an initial bias of −16 V, followed by +16, −16, and finally +16 V. In Fig. 5(a)–5(c) these domains are, respectively, identified to be 109°, 71°, 109°, and 71°, with respect to the unswitched region. The domain walls [Fig. 5(d)] labeled B–D are highly stable 180° walls, separating the 71°-switched and 109°-switched regions. Walls A and E are the relatively stable type I domain walls. The unlabeled domain walls at the sides are the less stable types II and IV, but they are significantly pinned by the much longer and more stable, neighboring domain walls. Thus it is expected that the entire switched region will retain its polarization structure over long durations. After 145 hours, the pattern is essentially unchanged (<6% change in area) unlike the simple pattern in Fig. 3, which completely relaxed in a few hours.

In conclusion, we demonstrate through a combination of phase-field modeling and scanning force microscopy of carefully controlled, epitaxial (110) BFO films that the polarization state can be altered by all three primary switching processes. Specifically, the instability of 109° switching processes has been dramatically reduced by a judicious combination of neighboring domain walls.

This work was supported by the Director, Office of Science, Office of Basic Energy Sciences, Materials Sciences and Engineering Division, of the US Department of Energy under Contract No. DE-AC02-05CH11231; NSF under No. DMR-0213623 and No. DMR-0507146; and by the Office of Naval Research under ONR Grant No. N00014-06-1-0008 and ONR-MURI Grant No. E-21-6RU-G4.

*To whom correspondence should be addressed.
yhchu@lbl.gov

[1] W. Eerenstein, N. D. Mathur, and J. F. Scott, Nature (London) **442**, 759 (2006).
[2] M. Fiebig *et al.*, Nature (London) **419**, 818 (2002).
[3] T. Lottermoser and M. Fiebig, Phys. Rev. B **70**, 220407 (2004).
[4] S. K. Streiffer *et al.*, J. Appl. Phys. **83**, 2742 (1998).
[5] A. E. Romanov *et al.*, J. Appl. Phys. **83**, 2754 (1998).
[6] P. Fischer *et al.*, J. Phys. C **13**, 1931 (1980).
[7] G. A. Smolenskii *et al.*, Sov. Phys. Solid State **2**, 2651 (1961).
[8] F. Kubel and H. Schmid, Acta Crystallogr. Sect. B **46**, 698 (1990).
[9] C. Michel *et al.*, Solid State Commun. **7**, 701 (1969).
[10] C. Ederer and N. A. Spaldin, Phys. Rev. B **71**, 060401(R) (2005).
[11] T. Zhao *et al.*, Nature Mater. **5**, 823 (2006).
[12] Y. H. Chu *et al.*, Adv. Mater. **19**, 2662 (2007).
[13] A. Gruverman, O. Auciello, and H. Tokumoto, Annu. Rev. Mater. Sci. **28**, 101 (1998).
[14] S. V. Kalinin and D. A. Bonnell, Phys. Rev. B **65**, 125408 (2002).
[15] F. Zavaliche *et al.*, Phase Transit. **79**, 991 (2006).
[16] L. Q. Chen, Annu. Rev. Mater. Res. **32**, 113 (2002).
[17] Y. L. Li *et al.*, Appl. Phys. Lett. **78**, 3878 (2001).